

HOT CORROSION BEHAVIOUR OF NICKEL CHROMIUM COATING AT DIFFERENT TEMPERATURES (800 °C AND 900 °C) ON SA213 T91 BOILER STEEL WELDMENTS

Rituraj Chandraker^{1*}, Anil Kumar², Rajesh Kumar³

¹Department of Mechanical Engineering, Chhatrapati Shivaji Institute of Technology,
Shivaji Nagar, Balod Road, Durg, 491001, Chhattisgarh, India

²Department of Mechanical Engineering Bhilai Institute of Technology,
Bhilai House, Durg, 491001, Chhattisgarh, India

³Department in Mechatronics Engineering, Chhatrapati Shivaji Institute of Technology,
Shivaji Nagar, Balod Road, Durg, 491001, Chhattisgarh, India

*e-mail: riturajchandrakar@csitdurg

Abstract. Hot corrosion is a serious problem in power generation equipment, gas turbines for ships aircrafts, energy conversion and chemical process systems. During combustion stage in heat engines, particularly in gas turbines, sodium and sulphur impurities present either in fuel or in combustion air, react to form sodium sulphate (Na_2SO_4). If the concentration of the sulphate exceeds the saturation vapour pressure at the operating metal temperature for turbine blades and vanes (700 °C-1100 °C), then deposition of the Na_2SO_4 will occur on the surface of these components. At higher temperatures the deposits of Na_2SO_4 are molten (melting point =884 °C) and can cause accelerating attack on high alloy or Cr-Mo steels. No alloy is immune to hot corrosion attack indefinitely, although there are some alloy compositions that require a long initiation time at which the hot corrosion process moves from the initiation stage to the propagation stage. Nickel-based coatings have been reported to be widely used as they combine several advantages such as abrasion, erosion and resistance to high-temperature corrosive atmospheres. In this report a comparison on the experimental performance of nickel-based coatings has been made to understand their hot corrosion mechanism.

1. Introduction

Materials are required to operate at high temperatures for several different reasons. In energy production systems, the conversion of chemical energy may be achieved by a heat engine, in which the heat of reaction of the fuel, typically reacting with oxygen, is converted first to mechanical energy, by way of a steam or gas turbine, or a reciprocating engine, and then to electrical energy by way of a generator. In a magneto hydrodynamic (MHD) system, the conversion to electricity is achieved by making the combustion gas electrically conducting, and passing it at high velocity through a magnetic field. In a fuel cell, the energy of the chemical reaction is again converted directly to electrical energy, and systems exist for doing this at room temperature. However, there are benefits in using higher-temperature systems. In chemical plant, high temperatures may be required to achieve specific reactions, or to increase reaction rates. Chromium molybdenum steel also referred to as heat resistant low alloy steel, find frequent application in power generation stations, refining, and chemical industries for

pressure vessels, piping systems, furnace components and rotating equipment. Elevated operating temperature usually taken to be higher than about 260 °C frequently required that weldment be produced of alloy steels because of the inferior hot strength and corrosion properties of carbon steels.

The type of weldments and its specific application dictates whether hot tensile strength, creep or stress rupture can be used as the basis of steel selection. The higher temperature corrosion problem may be complicated by other factors such as stress corrosion cracking, hydrogen attack etc. The use of alloys steels does not always control the corrosion of the weldments. Sometimes reduction of the service temperature/ or elimination of corrosive from the operating atmosphere are other means to alleviate this problem [1]. Ferritic chromium molybdenum steel are popular engineering alloys for a variety of moderate temperature, high pressure applications such as the steam generators/boilers of fossil-fuel and nuclear power plants, refining and processing of petroleum, high temperature high pressure vessels for thermal reforming and pressure vessels for coal liquefaction. Such steels possess a good combination of mechanical properties, formability and weldability, and resistance to high temperature oxidation and other forms of corrosion [2]. The materials used for high temperature applications are subjected to hot corrosion and high temperature wear. The corrosion is the deterioration of the materials by its reaction with surrounding and the rate increase in temperature known as hot corrosion. Hot corrosion is an accelerated oxidation of materials at elevated temperatures, induced by a thin film of fused salt deposit. In hot corrosion, metals and alloys are subjected to degradation at much higher rates than in gaseous oxidation, with porous non protective oxide scale problem in power generation equipments in gas turbines for ships and aircrafts and in other energy conversion and chemical process systems, because of the high thermodynamic stability of Na_2SO_4 , it is found to be common or dominant of the salt deposit [3]. Sulphur is a principal impurity in fossil fuels and sodium is introduced into the combustion air-usually in an aerosol originating from seawater. Some other alkali or alkaline sulphates may also exist in the deposit, depending upon the hot hard ware either from the condensation of combustion products of fossil fuels or else from the impingement of liquid droplets from the hot gas steam. The deposits often contain sulphates or chlorides with metallic constituents of Na, Ca, Mg, K, or V. the sources for these contaminants are the fuel and the air necessary for combustion. This type of degradation is especially severe when the condensed phase is liquid. Any welded components can be broadly divided into three different regions the weldments, the base metal, and the heat-affected zone (HAZ). The microstructures in these three regions are caused by different peak temperature and cooling rates. In fact, as one move away from the fusion line toward the base metal, one comes across sharp changes in the microstructures even within the HAZ due to different heating cycles experienced by the HAZ at different distances from the fusion line [4]. The oxidation behaviour of T-91 steel and T-22 steel in salt of 75 wt.% Na_2SO_4 + 25 wt.% NaCl has been studied under isothermal conditions at a temperature of 900°C in a cyclic manner. Oxidation kinetics was established for the T-91 steel and T-22 steel in salt at 900 °C under cyclic conditions for 50 cycles by thermo gravimetric technique. Each cycle consisted of 1 hour heating at 900 °C followed by 20 min of cooling in air. Both the samples nearly followed the parabolic rate law of oxidation. X-ray diffraction (XRD) and scanning electron microscopy/energy dispersive X-ray (SEM/EDAX) techniques were used to characterize the oxide scales. T-91 steel was found to be more corrosion resistant than T-22 steel under salt oxidation [5]. The concept of 'process maps' has been utilized to study the fundamentals of process-structure-property relationships in high velocity oxygen fuel (HVOF) sprayed coatings. Ni-20%Cr was chosen as a representing material of metallic alloys. In this paper, concurrent experiments including diagnostic studies, splat collection, and deposition of coatings were carried out to investigate the effects of fuel gas chemistry (fuel gas/oxygen

ratio), total gas flow, and energy input on particle temperature (T) and velocity (V), and coating microstructure formation and properties. Coatings were deposited on an 'in situ' curvature monitoring sensor to study residual stress evolution. A strong influence of particle velocity on induced compressive stresses through peening effect is discussed. The complete tracking of the coating buildup history including residual stress evolution and temperature deposition, in addition to single splat analysis allows the interpretation of resultant coating microstructures and properties, and enables coating design with desired properties [6]. Sachs (1958) studied accelerated high temperature corrosion of steel and stainless steel in V_2O_5 environment. They prepared that oxidation of pure Cr in V_2O_5 occurs with very rapid diffusion rate and so only the initial stage of the curve were reported to be more important. Later slowing down of the oxidation rate was attributed mainly to the effect of scale thickening. Loose and spongy appearance of the scale was observed by them at the beginning of the process; V_2O_5 was present in excess and did dissolve the products of oxidation [7]. The welded components of steel suffer deleterious micro structure degradation during welding. Since most of the in service failures are reported to occur in the HAZ, there have been extensive research efforts into correlating weld failures with some aspects of HAZ microstructure. The characteristics of the microstructures through weld zones and the size and extent of heat affected zones (HAZ) of weldment will depend on, among factors, the type of metals being joined whether or not they are heat treatable, and classes of welding or joining processes used. The objective of this study is to investigate the hot corrosion and high temperature oxidation behavior of boiler steel weldments in molten salt (Na_2SO_4 - 60% V_2O_5) corrosive environment especially at high temperature. Since it is found that in boiler operating such mixtures are often found to be responsible for boiler failures (weldment) [8].

2. Experimental procedure

It includes the procedure to obtain the weldments, their characterization, the hot corrosion studies and the analysis of final corrosion products. Filler material according to AWS E80-T5B3.

2.1 Nominal chemical composition for SA213 T91 boiler tube steel.

Table1. Chemical composition for SA213 T91 boiler tube steel.

Element	C	Mn	Si	V	Ni	Mo	Cr	Fe
Base metal	0.11	0.4	0.4	0.2	0.13	0.95	8.3	Balance

2.2 Execution of weldments.

A) Edge preparation.

The boiler tube was cut into approximation length of 100 mm each. Each tube was machined to obtained a single conventional V- groove, with 37.5° bevel angle for SA213 T91 steel with root and face 1mm as shown in Fig. 1.

B) Welding processes.

The plates were preheated to 200°C for $\frac{1}{2}$ hr. All weld joints were made by Gas tungsten Arc Welding (GTAW) process.

C) Formation of Weldments.

Prior to welding the boiler plate were thoroughly cleaned with brush and acetone so as to remove any oxide layer and dirt or grease adhering to the boiler plate. All process parameters including the root were constant throughout the welding process. The conditions were as reported in Table 2.

D) Preparation of Sample Materials.

The samples are cut in the Weld Zone (WZ) and Base Metal (BM). The samples were polished with 220 grit silicon carbide papers followed by 1/0, 2/0, 3/0, and 4/0 grade emery papers and finally wheel polished.

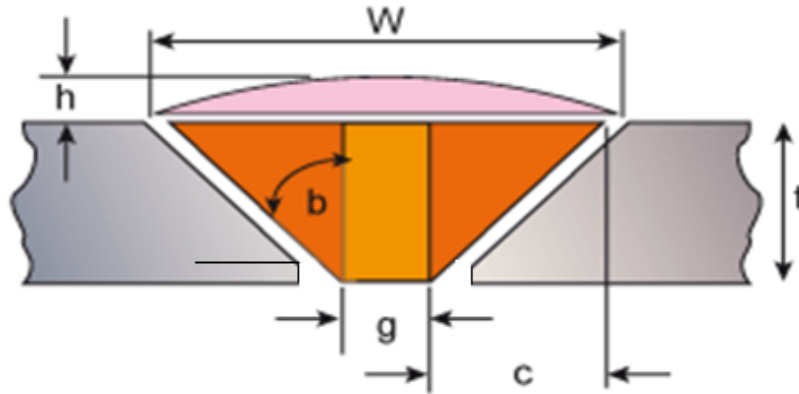


Fig. 1. Schematic view of weldment design for SA213 T91 boiler tube steel.
Here $t = 5 \text{ mm}$, $h = 3 \text{ mm}$, $b = 37.5^\circ$, $w = 15 \text{ mm}$, $g = 1 \text{ mm}$, $f = 1 \text{ mm}$.

Table. 2. Welding parameters for GTAW weldments.

Pre heating	200 °C
Joint design	single “V”
Shielding gas	Argon
Current	85 Amp
Voltage	16 Volts
Filler wire	TGS 9 CB
Plate thickness	5 mm
Gas flow rate	5 min ⁻¹

2.3 Characterisation of weldments.

A) Micro hardness Measurements.

The hardness data across the welds in the central region for both similar and dissimilar combinations are represented. The micro hardness of the weldment was measured using a ZWICK 3212 hardness testing. A load of 1000 gms (1 kg) was applied for duration of 15 sec. Hardness was measured at a distance of 1mm across the interface and 1mm along the base metal. Hardness survey was performed across the weld in the axial direction as well as along the weld in the radial direction. The maximum hardness was observed at interface of dissimilar weld metal, and minimum hardness was on the base metal side.

B) Metallographic studies.

For metallographic studies the weldments and unwelded samples were cut along the cross-section with diamond cutter (low speed saw, 04006, Buehler, USA make). The samples were polished by using SiC metallographic emery papers up to 1000 grit. After manual

polishing the samples were polished on high speed polishing wheel using diamond polishing series of 6 μm and 3 μm sizes. The final polishing is carried out on a sylvet-cloth using 1 μm size alumina powder suspension on polishing wheel machine. Sample was etched with picric reagent for 30 second, washed, dried and finally examined under MeF, Reichert-jung optical microscope made by Austria. The typical microstructures of the different regions of welded samples were photographed.

2.4 Hot corrosion studies.

A) Experimental setup.

Hot corrosion and oxidation studies were conducted at 800 °C and 900 °C for GTAW weldments in the laboratory silicon furnace, Digitech, India make. The furnace was calibrated with the variation of ± 5 °C using Platinum-Rhodium thermocouple and temperature indicator of Elecromek (Model-1551 P), India. Al_2O_3 boat was preheated up to 200 °C for hours with the assumption that its weight would remain constant during the cycle of study. The composite weldment, different regions of weldment and unwelded samples were subjected to mirror polishing following to wheel cloth polishing for 5 minutes before study. After polishing the samples were washed properly and dried in the hot air to remove the moisture. For every experiment the sample was kept in the boat, weight of boat and sample was measured before inserting in to the hot zone of the furnaces at 800 °C and 900 °C. The holding time in the furnace was one hour and after that the boat with sample was taken out and cooled at the ambient temperature for 20 minutes. Weight of the boat along with sample was measured and this constitutes one cycle. All hot corrosion and oxidation carried out for such 50 cycles. The weight change measurements were taken at the end of each cycle using an electronic weighing balance machine (Name of customer: MAARS DIGITECH SCALS) with a sensitivity of 0.1 mg.

B) Hot corrosion studies in molten salt (Na_2SO_4 - 60% V_2O_5).

I. Salt coating.

The unwelded and welded metal samples were heated in the oven up to 300°C and the salt mixture of Na_2SO_4 - 60% V_2O_5 dissolved in distilled water was coated on the warm polished samples with the help of camel hair brush. The amount of the salt coating varies from 3-5 mg/cm^2 . The coated samples were then dried at 200 °C for 3-4 hours in the oven and weighed along with the Al_2O_3 boat.

II. Hot corrosion studies.

The salt coated samples were subjected to hot corrosion in the laboratory in the furnace at 800 °C & 900 °C for 50 cycles. At end of each cycle critical observations were made regarding the corrosion products along with the weight change measurements.

2.5 Analysis of corrosion products of molten salt. All the samples subjected to hot corrosion were analyzed for the identification of corrosion products for both the surface as well as cross-section. The analysis was performed for surface and cross-section of corroded samples. Corroded samples were subjected to SEM/EDAX analysis.

A) Visual inspection.

Visual examination was made and recorded after each cycle for any change in color, luster, adherence-spalling tendency and development of crack in the scale etc. After the completion of 50 cycle (each cycle of 1 hr heating and 20 minutes cooling) in laboratory furnace and then their macroscopic views were taken.

B) Thermo gravimetric studies.

The weight change values were measured at the end of each cycle with the aim to understand the kinetics of hot corrosion and oxidation. The data was plotted with respect to number of cycles for each sample and the plots are given in the subsequent sections. In many cases splalling and scaling occurred in the alumina boat and the same is also added in the weight change values.

C) SEM/EDAX analysis.

Surface morphology. EDAX of corroded sample surfaces were performed at Sastra University Thanjaur (India) on JEOL (JSM-5 800) Scanning Electron Microscope with BSEM attachment of Oxford (Model-684 1) made in England on and its different regions samples. Samples were scanned under the microscope and critical areas of interests were photographed with an aim to identify the inclusions, micro racks and morphology of the surface scale. Thickness analysis was performed on various locations on these identified areas of interest on corroded surfaces of the samples with an aim to identify the various corrosion products.

3. Results

This paper deals with critical evaluation of the base steel and weldments obtained with GTAW welding process. The metallographic examinations of base steel as well the weldment have been discussed. The mechanical properties like micro hardness of weldment have been reported and discussed with respect to the existing literature.

3.1 Evaluation of microhardness of weldment. The hardness data across the welds in the central region for SA213 T91 weldments are presented in Fig. 2 the micro hardness of the weldment was measured using a ZWICK 3212 hardness testing. A load of 1000 gms (1 kg) was applied for duration of 15 sec. Hardness was measured at a distance of 1mm across the interface and 1mm along the base metal. Hardness survey was performed across the weld in the axial direction as well as along the weld in the radial direction. The maximum hardness was observed at interface of GTAW weld 500 HV.

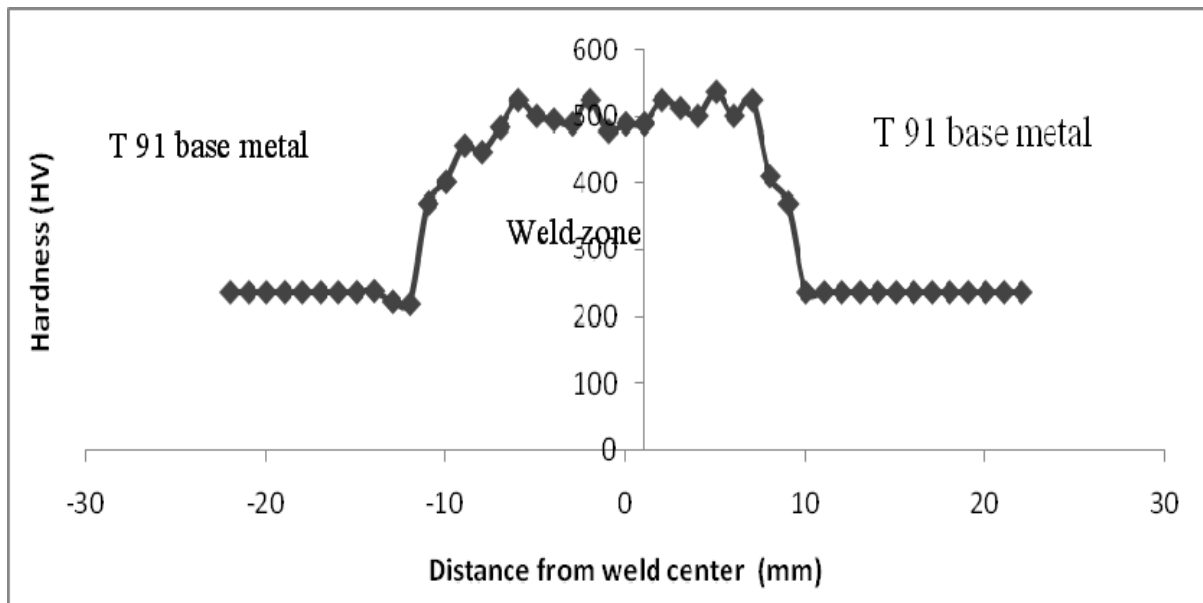


Fig. 2. Hardness distribution across the SA213 T91 GTAW weldment.

3.2 Metallographic studies.

A) Cross-sectional microstructure of GTAW weldment of SA213 T91 steel.

It was indicated by metallographic observation that the microstructure of T91 steel was tempering martensite and a small amount of fine grain ferrite as shown in Fig. 3.

Microstructure of the weld metal for T91 steel consists of austenite and a small amount of δ ferrite.

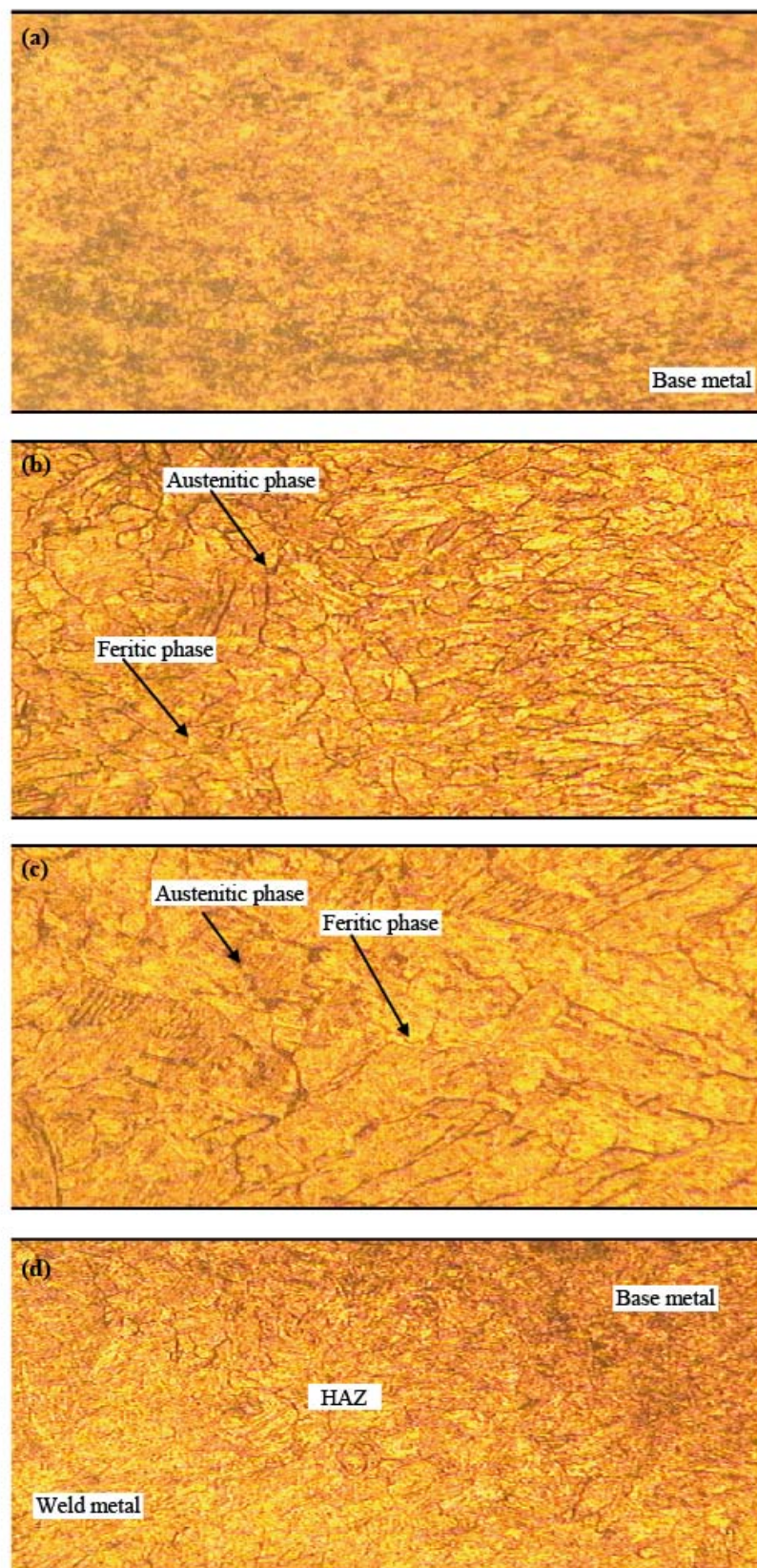


Fig. 3. Optical microstructures in the different region of the GTAW weldment of SA213 T91 boiler steel.
(a) Base metal, (b) HAZ zone, (c) weld metal.

3.3 Part (A). Hot corrosion studies of coated and uncoated weldments in molten salt environment at 800 °C. This deals with the critical examination of corrosion products and the behavior of weldments when subjected to hot corrosion at 800 °C under the thin coat of molten salt ($\text{Na}_2\text{SO}_4\text{-60\%V}_2\text{O}_5$) and high temperature environments at 800 °C with and without high temperature resistance coating. The samples were visually examined at the end of each cycle for in the color, luster, adherence of scale to the substrate and spalling tendency. The weight change measurements were made at the end of each cycle. Efforts have also been made to the mechanism of corrosion wherever possible.

Corrosion products were analyzed with the help of SEM/EDAX. The results for weldment have been reported under subheading. In view of comparison the thermo gravimetric data of welding process is plotted along with the unwelded steel. The parabolic rate constants values have been evaluated after 50 cycles of exposure.

A) *Different regions of GTAW weldment i.e. base metal and weld metal exposed to Molten Salt ($\text{Na}_2\text{SO}_4\text{-60\%V}_2\text{O}_5$) on coated and uncoated high temperature coating at 800 °C.*

I. Visual examination.

Macro morphology of the oxide scale for different regions of GTAW weldment after hot corrosion in $\text{Na}_2\text{SO}_4\text{-60\%V}_2\text{O}_5$ at 800 °C for 50 cycles is shown in Fig. 4. The color of substrate steels turned dull grey from dark brown during fifth cycle. Whereas in case of weld metal black color scale appeared on the whole surface from 3rd cycle itself and spalling of oxide scale in weldment has appeared around 15th cycle. Whereas the color of coated substrate steel was same as before during first cycle and in case of weld metal very dull grey color scale appeared on the whole surface from 1st cycle itself and spalling of oxide scale in weldment has appeared around 32th cycle.



Fig. 4. Different regions of coated GTAW weldment.

(a)Weld metal, (b) base metal exposed to molten salt ($\text{Na}_2\text{SO}_4\text{-60\%V}_2\text{O}_5$) at 800 °C for 50 cycles.

II. Thermo gravimetric data.

Weight change expressed in mg/cm^2 has been plotted in Figs. 5, 6 as a function of time expressed in number of cycles for the base metal and weldment of GTAW weldment in boiler steel at 800 °C. Total weight gain after 50 cycles of hot corrosion for weld metal is more than the total weight value of base metal in SA213-Gr91 boiler steel.

Table. 3. Parabolic rate constant K_p ($10^{-8} \text{g}^2 \text{cm}^{-4} \text{s}^{-1}$) of coated and uncoated GTAW weldments were exposed to Na_2SO_4 -60% V_2O_5 at 800 °C for 50 cycles.

Material	Uncoated	Coated
Base	6.079	0.734
GTAW weld	9.180	1.175

Parabolic equation:

$$x^2 = K_p t + C,$$

where, x is a weight gain rate, K_p is a rate constant, t is a time, C is a constant.

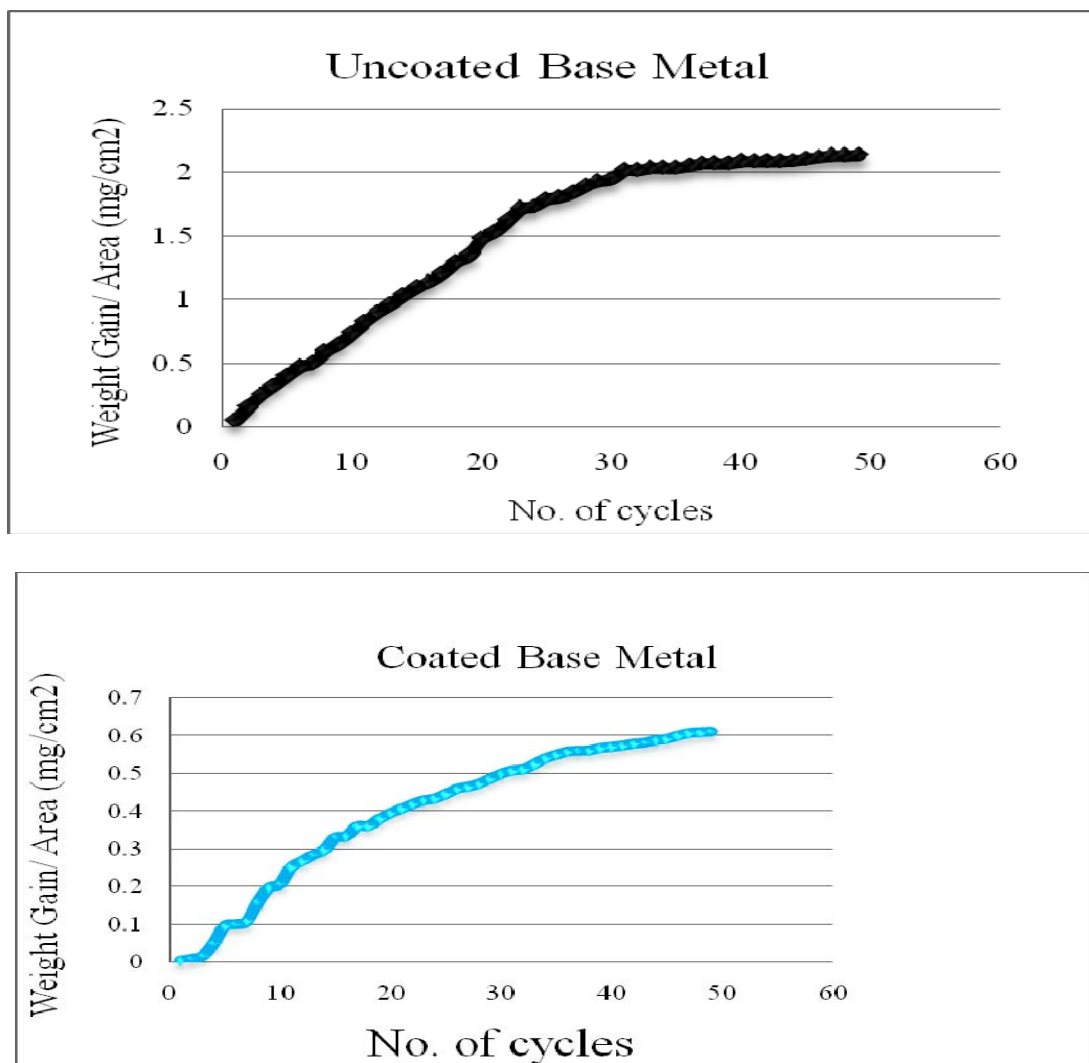


Fig. 5. Weight gain plot for different regions of coated and uncoated GTAW weldment exposed to Na_2SO_4 -60% V_2O_5 at 800 °C for 50 cycles.

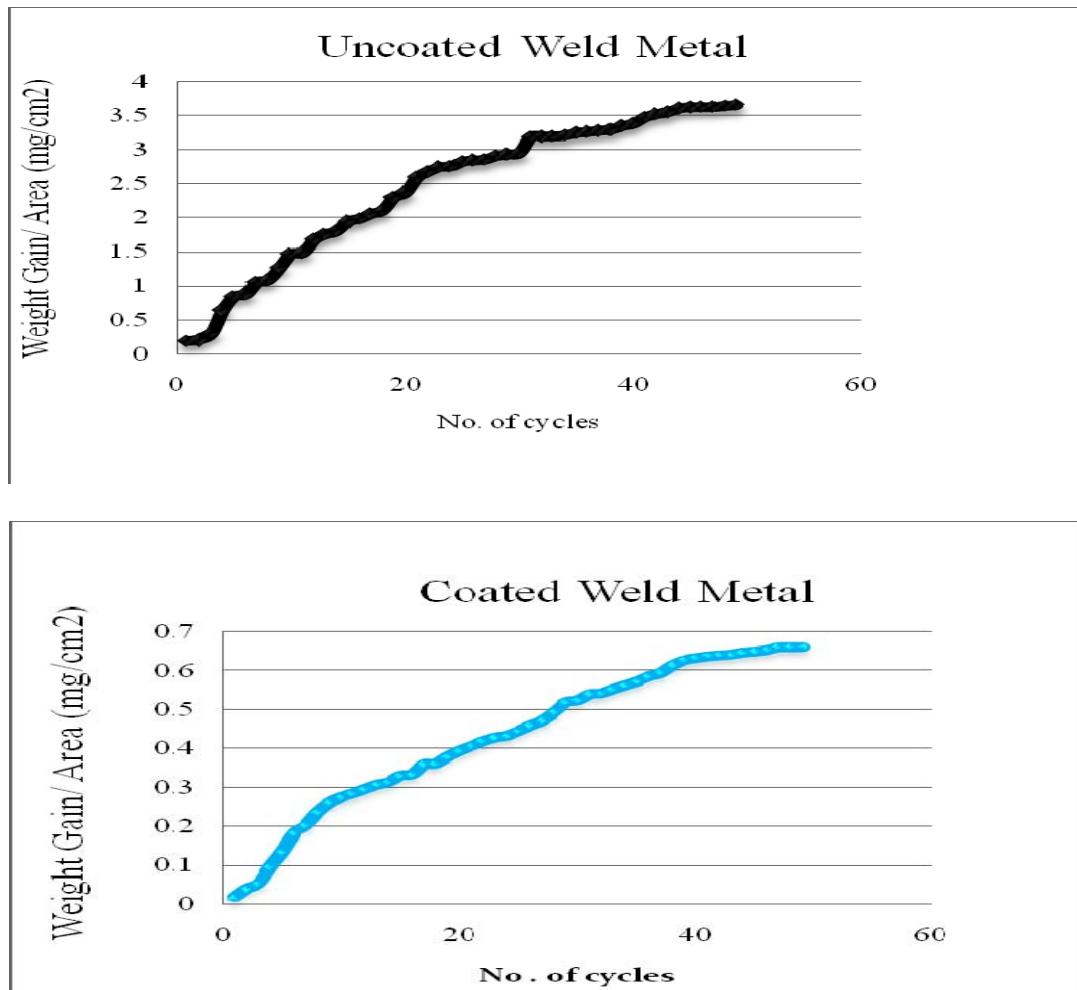


Fig. 6. Weight gain plot for different regions of coated and uncoated GTAW weldment exposed to Na_2SO_4 -60% V_2O_5 at 800 °C for 50 cycles.

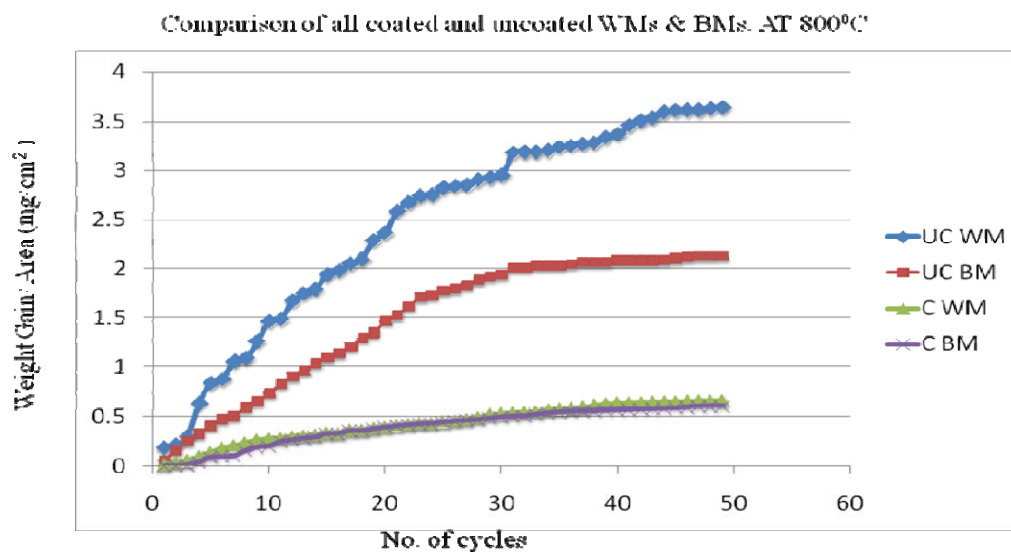
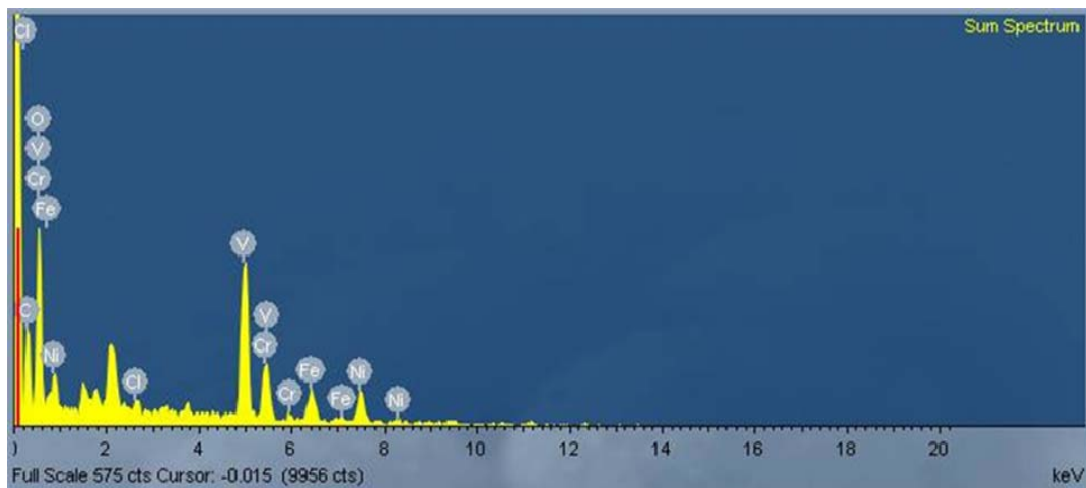
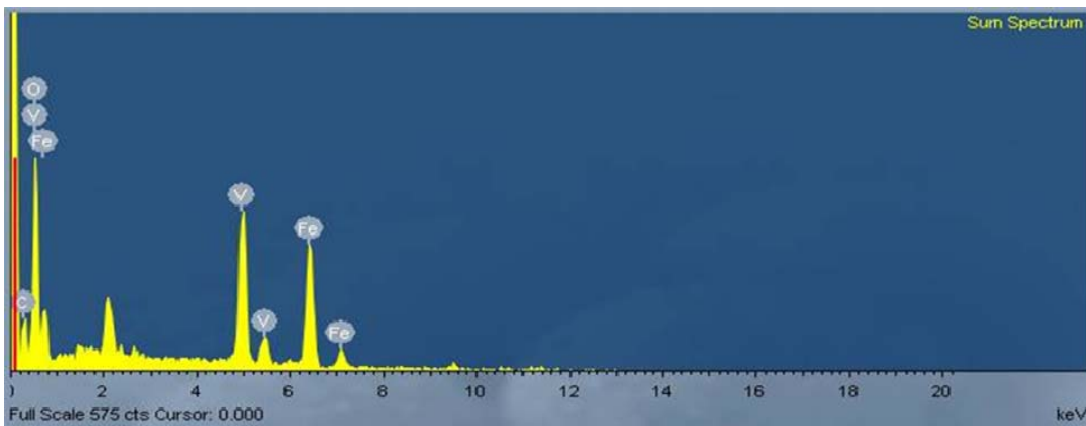


Fig. 7. Comparisons of all Weight gain plot for different regions of coated and uncoated GTAW weldment exposed to Na_2SO_4 -60% V_2O_5 at 800 °C for 50 cycles.

III. EDX analysis.



(a) Coated weldment



(b) Uncoated weldment

Fig. 8. Phase composition for coated and uncoated weld metal at 800 °C.

Table 4. Atomic % for coated weld metal at 800 °C.

Statistic	C	O	Cl	V	Cr	Fe	Ni
Mean	0.00	79.02	0.00	10.83	2.84	3.00	4.32
Std. dev.	0.00	0.00	0.00	0.00	0.00	0.00	0.00
Max.	0.00	79.02	0.00	10.83	2.84	3.00	4.32
Min	0.00	79.02	0.00	10.83	2.84	3.00	4.32

Results type: Decimal places:

(a) Atomic % of coated weldment

Table 5. Atomic % for uncoated weld metal at 800 °C.

Statistic	C	O	V	Fe
Mean	26.78	59.59	6.03	7.60
Std. dev.	0.00	0.00	0.00	0.00
Max.	26.78	59.59	6.03	7.60
Min	26.78	59.59	6.03	7.60

Results type : Decimal places :

(b) Atomic % of uncoated weldment

Table 6. Weight % for coated weld metal at 800 °C.

Processing option : All elements analysed (Normalised)

All results in weight%

Spectrum	In stats.	C	O	Cl	V	Cr	Fe	Ni	Total
Sum Spectrum Yes		0.00	53.02	0.00	23.14	6.19	7.02	10.63	100.00
Mean		0.00	53.02	0.00	23.14	6.19	7.02	10.63	100.00
Std. deviation		0.00	0.00	0.00	0.00	0.00	0.00	0.00	
Max.		0.00	53.02	0.00	23.14	6.19	7.02	10.63	
Min.		0.00	53.02	0.00	23.14	6.19	7.02	10.63	

(a) Wt % of Coated weldment

Table 7. Weight % for uncoated weld metal at 800 °C.

Processing option : All elements analysed (Normalised)

All results in weight%

Spectrum	In stats.	C	O	V	Fe	Total
Sum Spectrum Yes		16.03	47.51	15.31	21.15	100.00
Mean		16.03	47.51	15.31	21.15	100.00
Std. deviation		0.00	0.00	0.00	0.00	
Max.		16.03	47.51	15.31	21.15	
Min.		16.03	47.51	15.31	21.15	

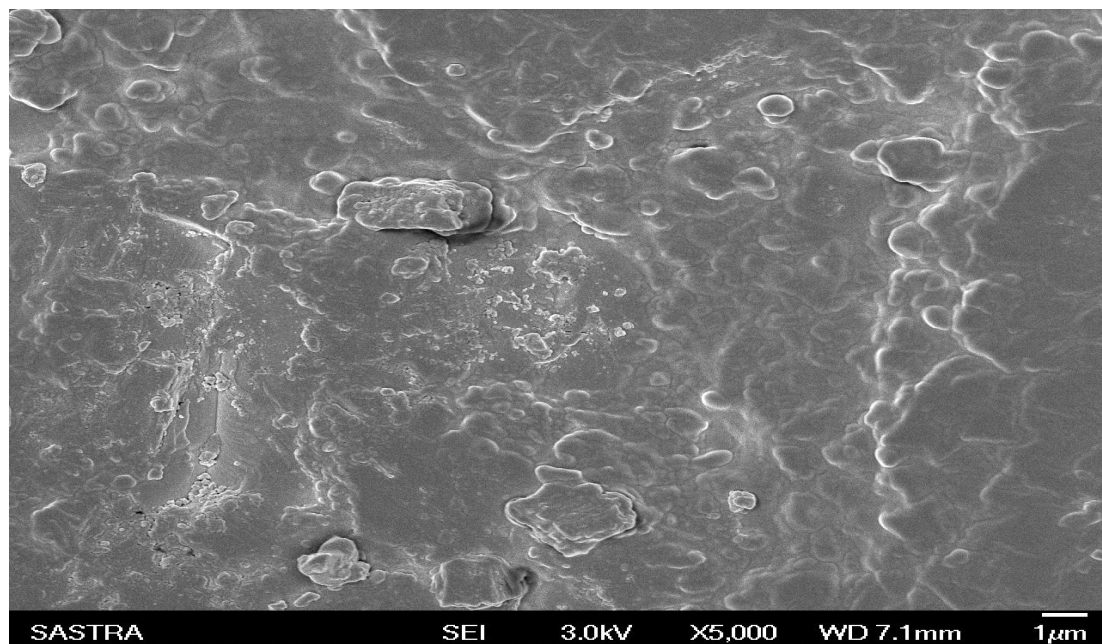
(b) Wt % of Uncoated weldment

IV. SEM analysis.

The surface SEM morphology of GTAW weldment and GTAW HAZ in T 91 boiler steel after cyclic oxidation in Na_2SO_4 -60% V_2O_5 at 800 °C is shown in Fig. 9.



(a)



(b)

Fig. 9. SEM analysis of coated GTAW weldment of T 91 subjected to cyclic Hot Corrosion in Na_2SO_4 - 60% V_2O_5 at 800 °C for 50 cycles.

(a) Base metal, (b) weld metal.

3.4 Part (B). Hot corrosion studies of coated and uncoated weldments in molten salt environment at 900 °C. This deals with the critical examination of corrosion products and the behavior of weldments when subjected to hot corrosion at 900 °C under the thin coat

of molten salt ($\text{Na}_2\text{SO}_4\text{-60\%V}_2\text{O}_5$) and high temperature environments at $900\text{ }^\circ\text{C}$ with and without high temperature resistance coating. The samples were visually examined at the end of each cycle for in the color, luster, adherence of scale to the substrate and spalling tendency. The weight change measurements were made at the end of each cycle. Efforts have also been made to the mechanism of corrosion wherever possible.

Corrosion products were analyzed with the help of SEM/EDAX. The results for weldment have been reported under subheading. In view of comparison the thermo gravimetric data of welding process is plotted along with the unwelded steel. The parabolic rate constants values have been evaluated after 50 cycles of exposure.

A) Different Regions of GTAW weldment i.e. Base Metal and Weld Metal exposed to Molten Salt ($\text{Na}_2\text{SO}_4\text{-60\%V}_2\text{O}_5$) on coated and uncoated high temperature coating at $900\text{ }^\circ\text{C}$.

I. Visual examination.

Macro morphology of the oxide scale for different regions of GTAW weldment after hot corrosion in $\text{Na}_2\text{SO}_4\text{-60\%V}_2\text{O}_5$ at $900\text{ }^\circ\text{C}$ for 50 cycles is shown in Fig. 10. The color of substrate steels turned more dull grey from dark brown during 3rd cycle as compared at $800\text{ }^\circ\text{C}$. Whereas in case of weld metal black color scale appeared on the whole surface from 1st cycle itself and spalling of oxide scale in weldment has appeared around 10th cycle. Whereas the color of coated substrate steel was same as before during first cycle and in case of weld metal very dull grey color scale appeared on the whole surface from 1st cycle itself and spalling of oxide scale in weldment has appeared around 24th cycle.

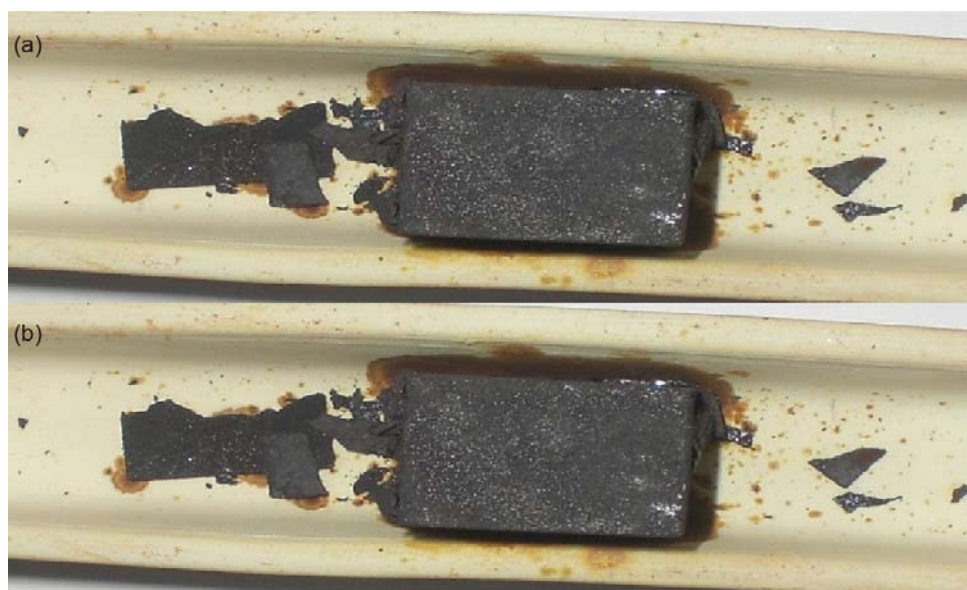


Fig. 10. Different Regions of GTAW coted weldment (a) base metal (b) weld metal exposed in molten salt environment at $900\text{ }^\circ\text{C}$ for 50 cycles.

II. Thermo gravimetric data.

Weight change expressed in g/cm^2 has been plotted in Figs. 11, 12 as a function of time expressed in number of cycles for the base metal and weldment of GTAW weldment in boiler steel at $900\text{ }^\circ\text{C}$. Total weight gain after 50 cycles of hot corrosion for weld metal is more than the total weight value of base metal in SA213-Gr91 boiler steel.

Table 8. Parabolic rate constant K_p ($10^{-8} \text{g}^2 \text{cm}^{-4} \text{s}^{-1}$) of coated and uncoated GTAW weldments were exposed to Na_2SO_4 -60% V_2O_5 at 90°C for 50 cycles.

Material	Uncoated	Coated
Base	10.103	2.416
GTAW weld	14.027	3.761

Parabolic equation:

$$x^2 = K_p t + C,$$

where, x is a weight gain rate, K_p is a rate constant, t is a time, C is a constant.

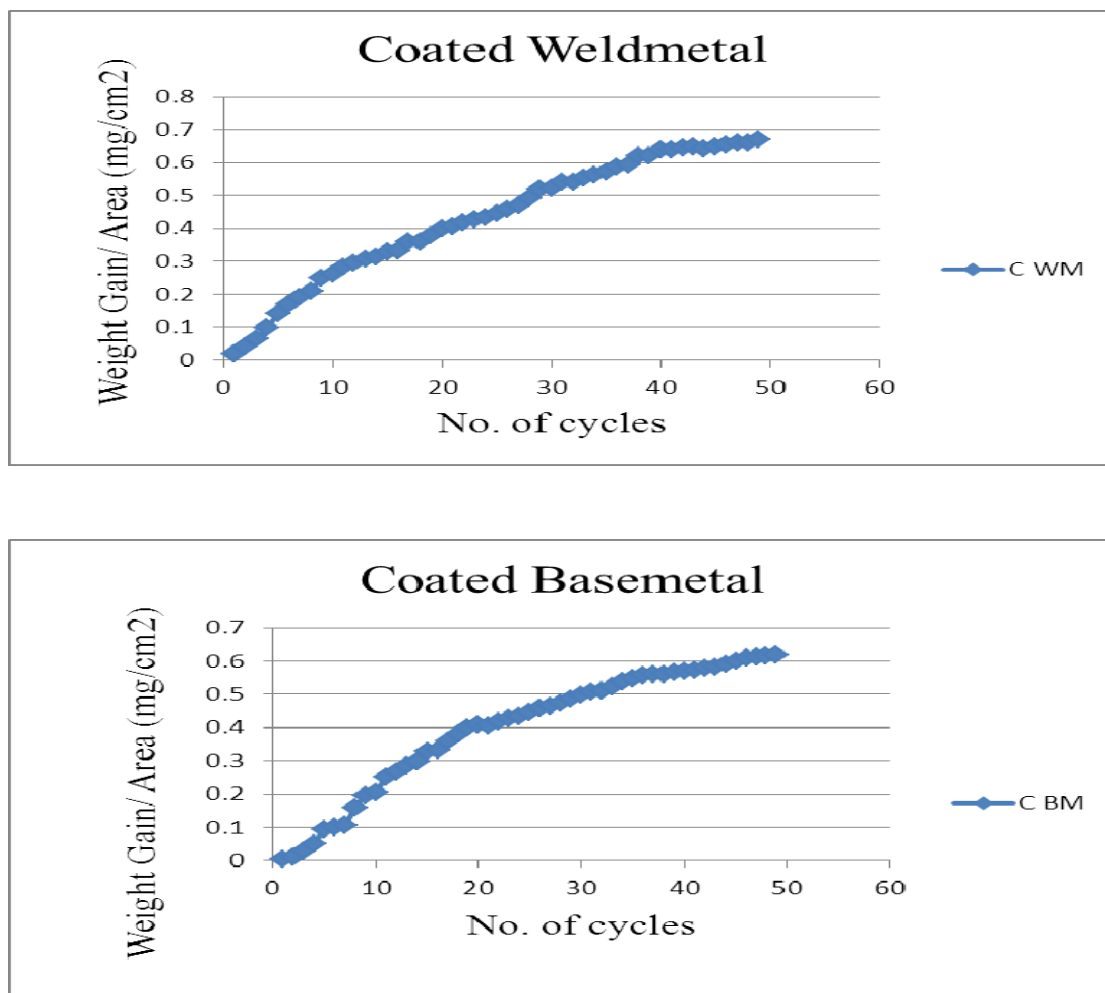


Fig. 11. Weight gain plot for different regions of coated and uncoated GTAW weldment exposed to Na_2SO_4 -60% V_2O_5 at 900°C for 50 cycles.

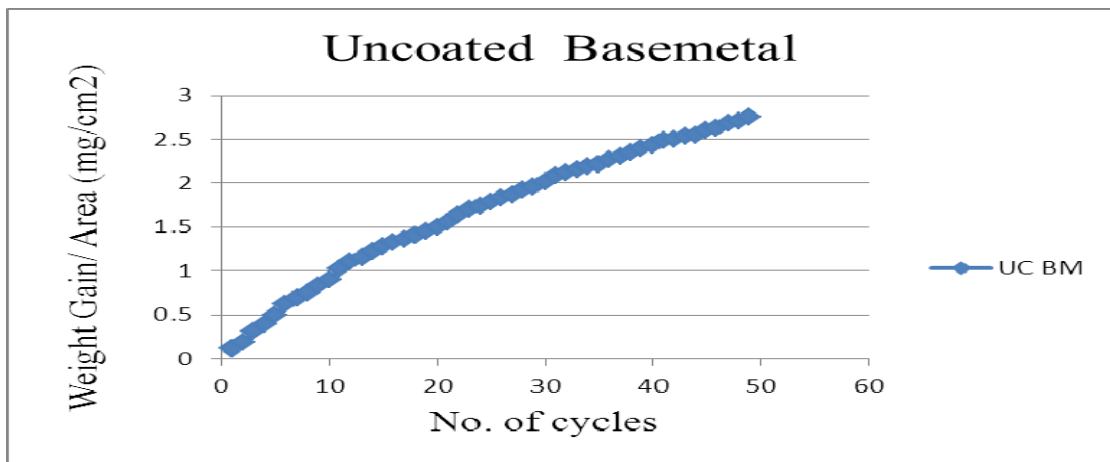
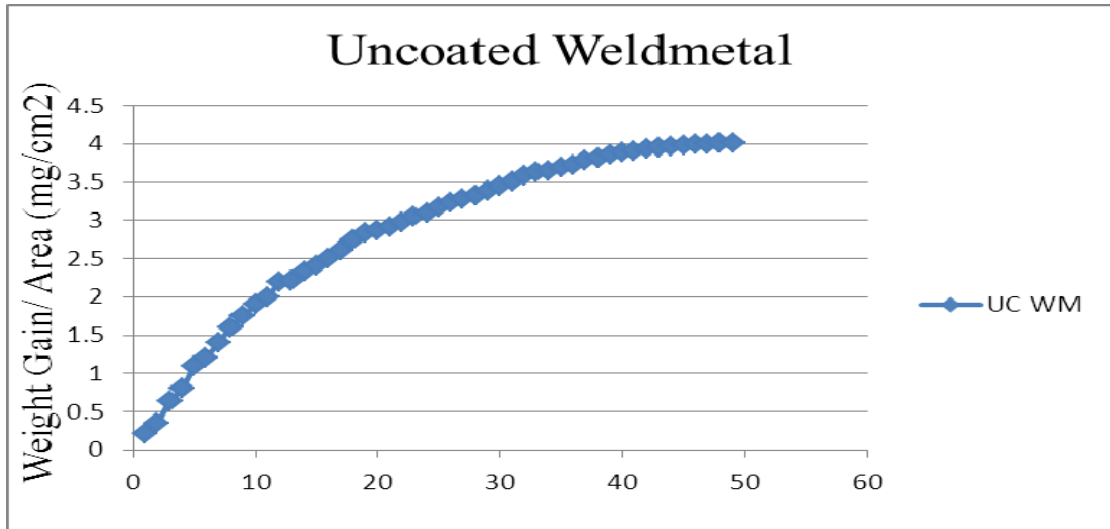


Fig. 12. Weight gain plot for different regions of coated and uncoated GTAW weldment exposed to Na₂SO₄-60%V₂O₅ at 900 °C for 50 cycles.

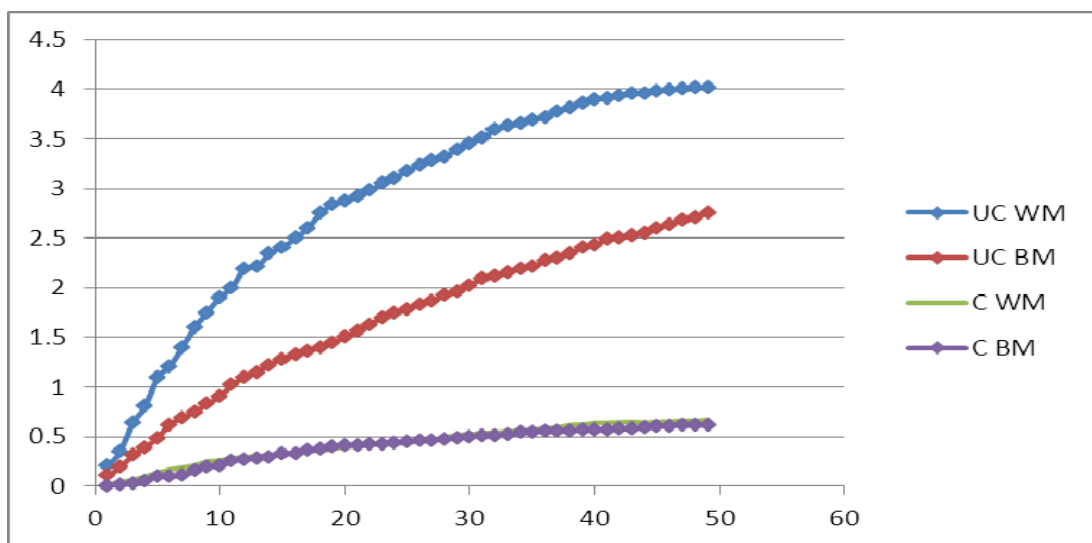
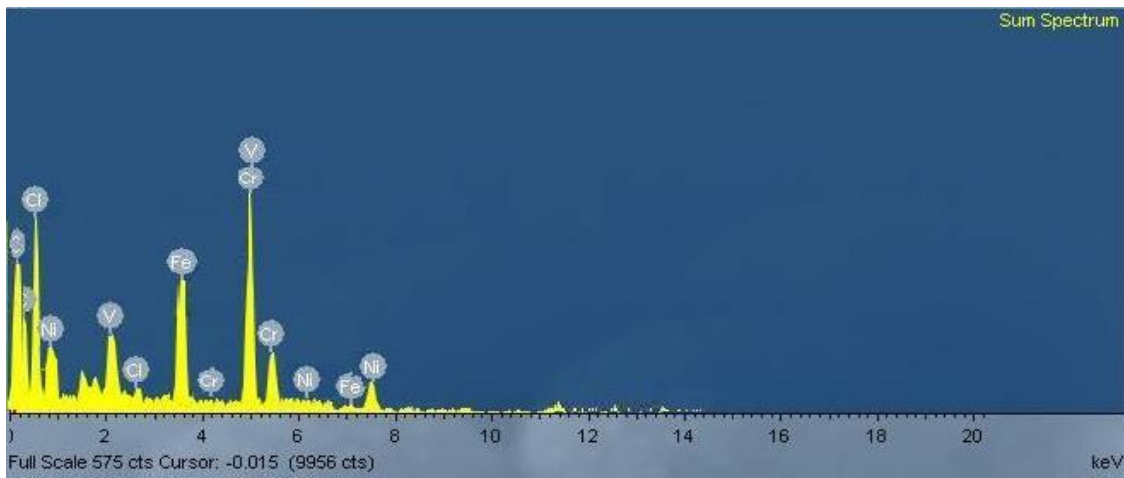
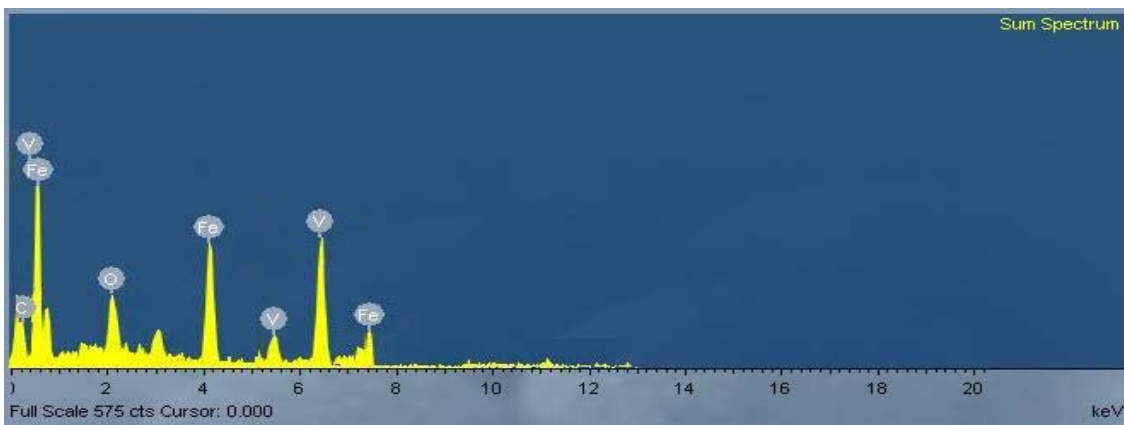


Fig. 13. Comparisons of all Weight gain plot for different regions of coated and uncoated GTAW weldment exposed to Na₂SO₄-60%V₂O₅ at 900 °C for 50 cycles.

III. EDX analysis.



(a) Coated weldment



(b) Uncoated weldment

Fig. 14. Phase composition for coated and uncoated weld metal at 900 °C.

Table 9. Atomic % for coated weld metal at 900 °C.

Statistic	C	O	Cl	V	Cr	Fe	Ni
Mean	0.00	77.72	0.00	11.02	2.98	3.13	5.15
Std. dev.	0.00	0.00	0.00	0.00	0.00	0.00	0.00
Max.	0.00	77.72	0.00	11.02	2.98	3.13	5.15
Min	0.00	77.72	0.00	11.02	2.98	3.13	5.15

Results type : Atomic% Decimal places : 2

Table 10. Atomic % for uncoated weld metal at 900 °C.

Statistic	C	O	V	Fe
Mean	26.78	59.59	6.03	7.60
Std. dev.	0.00	0.00	0.00	0.00
Max.	26.78	59.59	6.03	7.60
Min	26.78	59.59	6.03	7.60

Results type : Atomic% Decimal places : 2

Table 11. Weight % for coated weld metal at 900 °C.

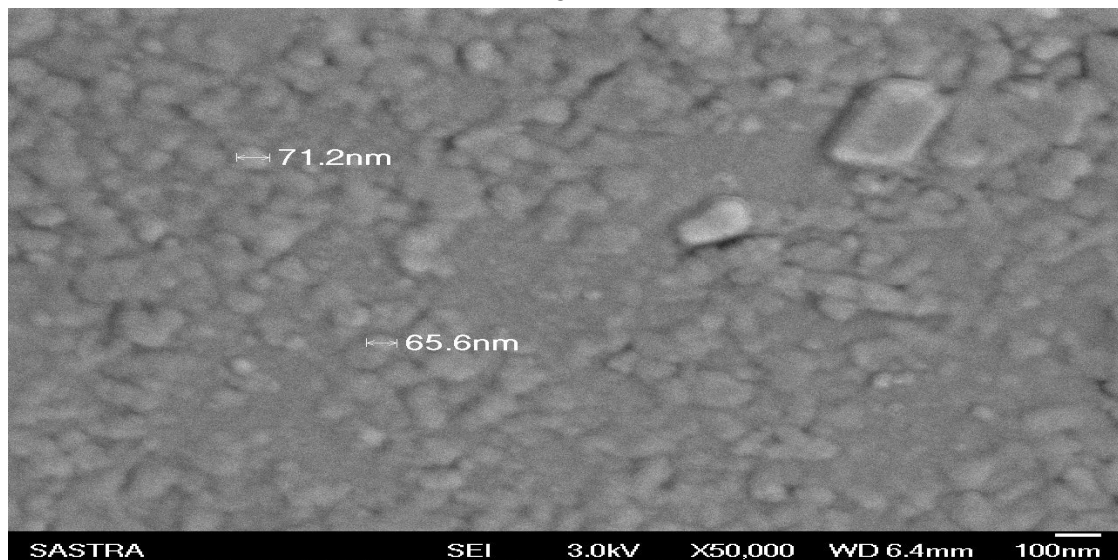
Spectrum	In stats.	C	O	Cl	V	Cr	Fe	Ni	Total
Sum Spectrum Yes		0.00	46.92	0.00	25.03	7.14	9.21	11.70	100.00
Mean		0.00	46.92	0.00	25.03	7.14	9.21	11.70	100.00
Std. deviation		0.00	0.00	0.00	0.00	0.00	0.00	0.00	
Max.		0.00	46.92	0.00	25.03	7.14	9.21	11.70	
Min.		0.00	46.92	0.00	25.03	7.14	9.21	11.70	

Table 12. Weight % for uncoated weld metal at 900 °C.

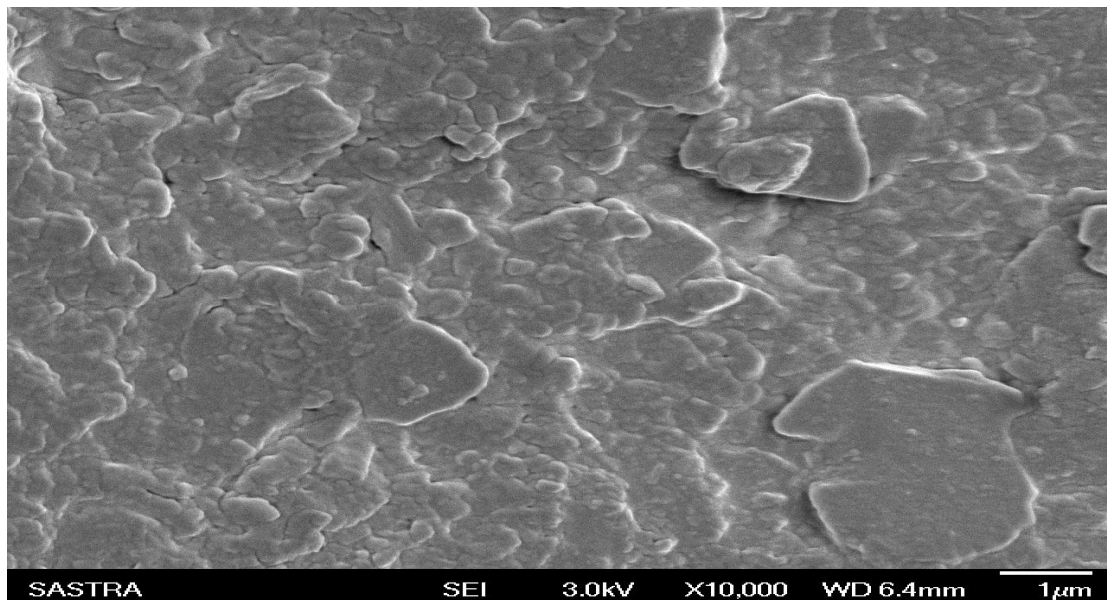
Spectrum	In stats.	C	O	V	Fe	Total
Sum Spectrum Yes		19.1	23.37	16.33	23.2	100.00
Mean		19.1	23.37	16.33	23.2	100.00
Std. deviation		0.00	0.00	0.00	0.00	
Max.		19.1	23.37	16.33	23.2	
Min.		19.1	23.37	16.33	23.2	

IV. SEM analysis.

The surface SEM morphology of GTAW weldment in T 91 boiler steel after cyclic oxidation in Na₂SO₄-60%V₂O₅ at 900 °C is shown in Fig. 15.



(a)



(b)

Fig. 15. SEM analysis of uncoated GTAW Weldment of T 91 subjected to cyclic Hot Corrosion in Na_2SO_4 - 60% V_2O_5 at 900 °C for 50 cycles.

(a) Base metal, (b) GTAW weldment.

4. Conclutions

Micro hardness measurement across the cross section of weldments for GTAW showed that the weld region is having higher hardness compared to the HAZ and base regions. This difference in harness was attributed to the formation of carbides during weld thermal cycle.

There is not much difference in wt. gain rate between 800 °C and 900 °C temperature. This may be because of the melting temperature of the Na_2SO_4 .

There is a negligible wt. gain difference for coated weldments at 800 °C and 900 °C.

Atomic and weight percentage of iron is more in uncoated specimen as compared to the coated specimen because of the nickel chromium coated layer in coated specimen which reduces spllation of the surface.

Percentage of vanadium as well as iron increases as temperature increases due to more kinetic of corrosion. GTAW weld region showed more weight gain compared to all specimens when subjected hot corrosion, which may be due to presence of oxides and spinels of manganese and chromium. The base metal shows less weight gain.

In the earlier stages of high temperature corrosion there is a rapid increase in weight gain for all specimens which may be due to the rapid pick oxygen pick up by diffusion of oxygen through the molten layer.

Intensive spalling of the scale observed at high temperature corrosion can be attributed to severe strain developed because of Fe_2O_3 precipitation from the liquid phase and inter diffusion of the intermediate layer of iron oxide.

Nickel based coatings such as Ni–Cr have been found to exhibit excellent hot corrosion resistance.

Vanadate compounds are good oxidation catalysts and allow oxygen and other gases in the combustion atmosphere to diffuse rapidly to the metal surface and cause further oxidation. As soon as the metal is oxidized, the cycle starts over again and high corrosion rates occur.

References

- [1] J.E. Indacochea // *Key Engineering Materials, Trans. Tech. publication* **69-70** (1992) 47.
- [2] H. B Cary, *Modern Welding Technology* (Practice Hall, Inc., Englewood Cliffs, N.J., 1979).
- [3] E. Otero, A. Pardo, J. Hernaez, F.J. Perez // *Corrosion. Sci.* **34** (1992) 1747.
- [4] P.J. James, L.W. Pinder // *Materials at Temperatures* **14** (1997) 187.
- [5] Dinesh Gonda, Vikas Chawlab, D. Puria, S. Prakash // *Journal of Minerals and Materials Characterization and Engineering* **9** (2010) 593.
- [6] A. Valarezo, W.B. Choi, W. Chi, A. Gouldstone, S. Sampath, In. *Conference Paper from Thermal Spray 2007: Global Coating Solutions (ASM International)*, <http://www.corrosionanalysisnetwork.org/portal/site/csc/template.PAGE>.
- [7] Harpreet Singh, Devendra Puri, Satya Prakash // *Rev. Adv. Mater. Sci.* **16** (2007) 27.
- [8] T.S. Sidhu, S. Prakash, R.D. Agrawal // *Current Science* **90** (2006) 41.
- [9] R. Kumar, V.K. Tewari, S. Prakash // *Metallurgical and Materials Transaction A* **38** (2007) 54.
- [10] Dionisio Laverde, Tomás Gómez-Acebo, Francisco Castro // *Corrosion Science* **46** (2004) 613.
- [11] Chun-Hao Koo, Ching-Yuan Bai, Yi-Jun Luo // *Materials Chemistry and Physics* **86** (2004) 258.
- [12] M.F. Montemor, M.G.S. Ferreira, N.E. Hakiki, M. Da Cunha Belo // *Corrosion Science* **42** (2000) 1635.
- [13] R.K. Singh Raman, B.C. Muddle // *International Journal of Pressure Vessels and Piping* **77** (2000) 117.
- [14] Pi-Chuen Tsai, Chen-Sheng Hsu // *Surface and Coatings Technology* **183** (2004) 29.